Cell, Vol. 122, 85–95, July 15, 2005, Copyright ©2005 by Elsevier Inc. DOI 10.1016/j.cell.2005.04.025

Contribution of the Endoplasmic Reticulum to Peroxisome Formation

Dominic Hoepfner,[1,2] Danny Schildknegt,[1] Ineke Braakman,[1] Peter Philippsen,[2] and Henk F. Tabak[1,3,4,*]
[1]Department of Cellular Protein Chemistry
University of Utrecht
Padualaan 8
NL-3548 CH Utrecht
The Netherlands
[2]Lehrstuhl für Angewandte Mikrobiologie
Biozentrum
Universität Basel
Klingelbergstrasse 70
CH-4056 Basel
Switzerland
[3]Laboratory of Cell Biology
University Medical Center Utrecht
Heidelberglaan 100
NL-3584 CX Utrecht
The Netherlands
[4]Academic Biomedical Centre
University of Utrecht
Yalelaan 1
NL-3548 CL Utrecht
The Netherlands

Summary

How peroxisomes are formed in eukaryotic cells is unknown but important for insight into a variety of diseases. Both human and yeast cells lacking peroxisomes due to mutations in *PEX3* or *PEX19* genes regenerate the organelles upon reintroduction of the corresponding wild-type version. To evaluate how and from where new peroxisomes are formed, we followed the trafficking route of newly made YFP-tagged Pex3 and Pex19 proteins by real-time fluorescence microscopy in *Saccharomyces cerevisiae*. Remarkably, Pex3 (an integral membrane protein) could first be observed in the endoplasmic reticulum (ER), where it concentrates in foci that then bud off in a Pex19-dependent manner and mature into fully functional peroxisomes. Pex19 (a farnesylated, mostly cytosolic protein) enriches first at the Pex3 foci on the ER and then on the maturing peroxisomes. This trafficking route of Pex3-YFP is the same in wild-type cells. These results demonstrate that peroxisomes are generated from domains in the ER.

Introduction

For eukaryotic cells, it is essential to maintain and inherit their set of organelles during proliferation. To achieve this, a number of criteria need to be met: growth of organelles by recruitment of newly synthesized proteins, enlargement of membrane surface, division to increase organelle numbers, and partitioning between the two progeny cells. These general steps are not equally executed by all organelles, which may be a reflection of their evolutionary past. Some organelles, such as the Golgi complex, endosomes, and lysosomes (vacuoles), are in permanent dynamic equilibrium and, upon loss, can be derived from the ER, the compartment from which they originate. Other organelles, such as mitochondria, chloroplasts, and the endoplasmic reticulum (ER), are considered as autonomous entities. Loss of any of these organelles is permanent and fatal for the cell, since no means exist to regenerate them again (reviewed by Nunnari and Walter, 1996; Warren and Wickner, 1996). How do peroxisomes, small and abundant organelles containing mostly oxidases producing reactive oxygen species (van den Bosch et al., 1992), fit into this picture?

Peroxisomes could thus far not unambiguously be classified to either group of organelles. Suggestions to classify peroxisomes together with mitochondria and chloroplasts are based on two considerations: (1), the observation that most peroxisomal proteins, particularly the ones present in the matrix space of the organelle, are synthesized on free polyribosomes and imported directly from the cytosol into the organelle (reviewed by Lazarow and Fujiki, 1985) and (2), the supposition that peroxisomes evolved from an endosymbiont during evolution (de Duve, 1996). However, an observation at odds with peroxisomes being such autonomous organelles is their remarkable property of regeneration. Fibroblasts of human patients or yeast mutants lacking peroxisomes regenerate peroxisomes after complementation with the wild-type version of the mutated gene (reviewed by Subramani, 1998). Thus, even after cultivating such mutants for many generations without peroxisomes, cells manage to reform them without much delay. The crucial events of this process have never been observed, however. Taking into account the aphorism "omnis membrana ex membrana" (Günther Blobel, Nobel Prize 1999), the question arises of which membrane serves as the donor for the regeneration of these new peroxisomes.

In the past, EM pictures have been published in which peroxisomes were observed in close association with the ER or in which membrane continuities between peroxisomes and the ER were seen (Novikoff and Novikoff, 1972). For lack of biochemical evidence backing up these electron-microscopical observations, the concept of an ER contributing to peroxisome formation never met wide acceptance (Lazarow and Fujiki, 1985). Recently, we have confirmed and extended these old electron-microscopic observations using modern immunogold labeling techniques to positively identify stages in peroxisome development and electron tomography to make three-dimensional reconstructions of them (Geuze et al., 2003; Tabak et al., 2003).

Here we have taken a closer look at the crucial moments when peroxisomes reappear on the scene. We have developed kinetic assays, combining real-time fluorescence microscopy and biochemistry, to establish a

*Correspondence: h.f.tabak@chem.uu.nl

precursor to the product relationship for two proteins, Pex3 and Pex19, that function at an early stage of peroxisome development. Pex3 is an integral membrane protein (Höhfeld et al., 1991), and Pex19 is a mostly cytosolic protein with a farnesylated tail (Götte et al., 1998). Both proteins are involved in directing most of the peroxisomal-membrane proteins to their correct location (Fang et al., 2004; Jones et al., 2004; Sacksteder et al., 2000). Pex19 was shown to bind to various membrane proteins via a small consensus amino acid sequence (Jones et al., 2004; Rottensteiner et al., 2004). It physically interacts with Pex3, which is suggested to anchor the Pex19-cargo complex to the acceptor membrane (Fang et al., 2004; Götte et al., 1998). Interestingly, mutation of either one of these genes results in yeast or mammalian cells completely lacking peroxisomes, thus ranking Pex3 and Pex19 at the hierarchical top of the peroxisome biogenesis pathway (reviewed by Schliebs and Kunau, 2004).

We have introduced the wild-type *PEX3* or *PEX19* gene under the control of the *GAL1* promoter in a *pex3Δ* or *pex19Δ* mutant of *S. cerevisiae*. After induction of the wild-type genes, we have followed trafficking of the newly synthesized YFP-tagged Pex3 or Pex19 proteins using real-time imaging in living cells. The wild-type phenotype, which is characterized by the presence of multiple protein-import-competent peroxisomes, is restored within 5 hr after induction. Interestingly, both Pex3 and Pex19 proteins appear first in the ER before maturing into peroxisomes. In addition, Pex3- and Pex19-labeled foci initially localize to the ER before maturing into ER-independent, import-competent peroxisomes. These results suggest that the ER contributes to peroxisome formation, particularly by donating lipid material for the peroxisomal membrane and thus classifying peroxisomes into the group of ER-derived organelles.

Results

Reformation of Peroxisomes: Experimental Setup

We have assessed how peroxisomes are formed using genetically modified *S. cerevisiae* strains that express different fluorescently labeled marker proteins allowing real-time imaging analysis of peroxisome biogenesis. The experimental system involves a strain carrying *PEX3* solely under the control of the inducible *GAL1* promoter. In the absence of galactose, Pex3 is absent and the cells display the published mutant phenotype, cells without peroxisomes (Erdmann et al., 1989; Hettema et al., 2000; Höhfeld et al., 1991). The complete absence of peroxisomal membrane structures could be confirmed by the diffuse cytoplasmic localization of an integral peroxisomal-membrane protein (Pex15) and a peroxisomal-membrane-associated protein (Pex1) (see Figure S1 in the Supplemental Data available with this article online). A disadvantage of the *GAL1* promoter is the high Pex3 protein level obtained after induction, which can lead to mislocalization and hampers normal peroxisome development and maintenance. We therefore exposed the cells to galactose for 30 min only, followed by glucose to repress the promoter again. The amount of Pex3 protein produced during the 5 hr that we monitored the cells compares well with the steady-state level of Pex3 protein produced from the endogenous promoter (Figure 1). After 3 hr, this level drops because cells continue to multiply during the course of the experiment. Accordingly, 5 hr after the limited induction, we observed the appearance of newly formed peroxisomes indistinguishable from wild-type in terms of number, localization, and potential to import peroxisome-targeting signal 1 (PTS1) containing proteins (compare Figure 2, 300 min and Figure S2).

To follow the trafficking route of Pex3 during the peroxisome biogenesis period, we have analyzed and compared two strains with Pex3-YFP under control of the *GAL1* promoter as the only source of Pex3. To illustrate whether or not the ER is an intermediate compartment in the route of Pex3 to its final destination, one strain (DHY552) constitutively expresses Sec63-CFP to visualize the ER (Fehrenbacher et al., 2002). To illustrate when peroxisomes reappear that are capable of importing PTS1-containing proteins and to indicate when Pex3 arrives at its final destination, the other strain (DHY553) constitutively expresses CFP-PTS1. To decrease the chance of coincidental colocalization, we used diploid cells, as they are larger and therefore more suitable for microscopy. A detailed description of the genetic setup is depicted in the table describing the strains (see Table S1).

Using these two strains, we induced peroxisome reformation in cells devoid of this organelle and followed Pex3-YFP from its first appearance until restoration of wild-type peroxisomes 5 hr later.

Pex3-YFP Travels via the ER to Peroxisomes

Figure 2A shows characteristic time points of the developmental process triggered by limited induction of Pex3-YFP in strain DHY552. At all time points, the perinuclear and cortical ER is clearly visible (Sec63-CFP). At time 0, no Pex3-YFP is present, but 1 hr after induction, the first Pex3-YFP fluorescence appears in subcellular structures overlapping with the Sec63-CFP-marked ER. Most of the ER in *S. cerevisiae* is perinuclear, and particularly revealing in this respect, therefore, are the bilobed nuclear anaphase structures present in dividing cells. Ninety minutes later, ER-localized Pex3-YFP fluorescence concentrates in one or two dots per cell that are still associated with the ER. After 2 hr, the first Pex3-YFP dots were detectable that no longer showed colocalization with Sec63-CFP. Finally, after 5 hr, we observed multiple, small dots per cell that show no association with the ER but represent the punctate-fluorescence picture typical of the presence of peroxisomes (for comparison, see Figure S2).

The other strain, DHY553, illustrates these findings in a different way (Figure 2B). At all time points CFP-PTS1 is produced. Initially, no structures are present that can incorporate CFP-PTS1, and cells present overall fluorescence, illustrating CFP-PTS1's cytosolic location. After 2 hr, the first subcellular accumulations can be observed in some cells showing one or two fluorescent specks that colocalized with the Pex3-YFP dots, indicating that the Pex3-YFP-labeled structures matured into PTS1-protein-import-competent peroxisomes. Af-

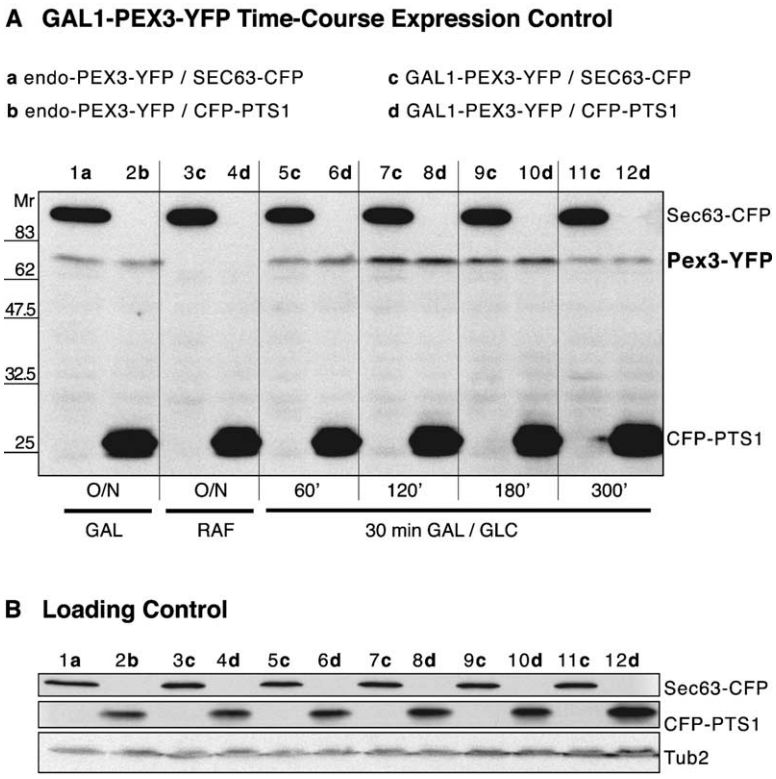

Figure 1. Comparison of Pex3-YFP Production from the Endogenous and the *GAL1* Promoter

(A) Equal amounts of protein extracted from strains with Pex3-YFP under the endogenous promoter (a and b) and under the control of the *GAL1* promoter (c and d) were separated by SDS-PAGE and subjected to immunoblot analysis with antibodies against GFP. The antibody recognized the 77 kDa Pex3-YFP fusion protein, the 95 kDa Sec63-CFP (a and c), and the 27 kDa CFP-PTS1 protein (b and d). The first two lanes from the left show Pex3-YFP steady-state levels expressed from the endogenous promoter. Lanes 3 and 4 show absence of Pex3-YFP under control of the *GAL1* promoter in cells grown on raffinose. Lanes 6–12 show time points of limited Pex3-YFP induction from the *GAL1* promoter. The promoter was induced for 30 min on galactose only, followed by renewed repression on glucose. Samples were taken at 60, 120, 180, and 300 min. The blot was exposed for 60 min.

(B) Loading control. Short, 1 min exposures of the Sec63-CFP signal as well as the CFP-PTS1 signal allow verification that equal amounts of protein from the corresponding strains have been loaded. In addition, the blot was stripped and reprobed with an antibody against β-tubulin (Tub2). This blot was exposed for 60 min.

ter 5 hr, formation of peroxisomes is complete, and CFP-PTS1 presents the multipunctate fluorescence typical of wild-type cells (for comparison, see Figure S2).

Controls were carried out to validate the experimental setup and the results obtained. We added cycloheximide 60 min after induction of the *GAL1* promoter (30 min after the glucose block) to inhibit further protein synthesis. The signal strength of Pex3-YFP produced is similar to that of uninhibited cells. It indicates that the glucose block is efficient and that we are dealing with a real pulse-chase situation. However, in the late stage of the 4 hr observation period, some component becomes limiting due to the overall inhibition of protein synthesis and the appearance of CFP-PTS1 import-competent organelles is diminished (for experimental procedures and further details, see Figure S3). One hour after induction, when newly synthesized Pex3-YFP is present in the ER, cells were bleached with light in the YFP channel. This resulted in almost complete loss of the ER-Pex3-YFP signal. Restoration of fluorescence in the ER did not take place, and only very weak fluorescence (<10% of the control) could be observed in a few dot-like structures. Nevertheless, 300 min after induction, all cells show CFP-PTS1-fluorescent peroxisomes. We found no evidence for a separate non-ER-associated pool of Pex3-YFP, such as a putative "protoperoxisome" (Lazarow, 2003; Bascom et al., 2003), that could have served as initiator of peroxisome formation (for experimental procedures and further details, see Figure S4). The experiments reported in Figure 2 have been repeated with a mutant form of YFP (L221K) that shows no self-interaction to exclude negative side effects of possible self-association, such as aggregation (Phillips, 1997; Zacharias et al., 2002; Lisenbee et al., 2003). Results with these strains (DHY889 and DHY892) were identical to the results shown in Figure 2 (data not shown). Finally, we made a time-lapse series over a short period with 10 min intervals to show that the first dot-like structures formed are indeed derived from the ER (for experimental procedures and further details, see Figure S5). All these data are compatible with one pool of Pex3-YFP that first appears in the ER and subsequently transfers via dot-like structures into mature peroxisomes and leave no room for the concept of a putative protoperoxisome (Lazarow, 2003; Bascom et al., 2003).

We also assessed the arrival of Pex3 shortly after synthesis in the ER in a biochemical fashion. We have made use of the observation that the position of ER-derived vesicles in an equilibrium density gradient depends on the Mg^{2+} concentration in the medium (Roberg et al., 1997). In a *GAL1-PEX3-YFP SEC63-CFP CFP-PTS1* strain (DHY739), we induced Pex3 as described above. At the 90 min time point, when Pex3-YFP colocalizes with Sec63-CFP (Figure 2A), the cells were prepared for equilibrium-density-gradient centrifugation. Fractionation of a postnuclear supernatant was performed in sucrose gradients containing either 1 mM Mg^{2+} or 10 mM EDTA, and the gradients were spun to equilibrium. Fractions were collected, separated by gel electrophoresis followed by Western blotting, and probed with an anti-GFP antibody. In this way, three different proteins can be differentiated on the basis of

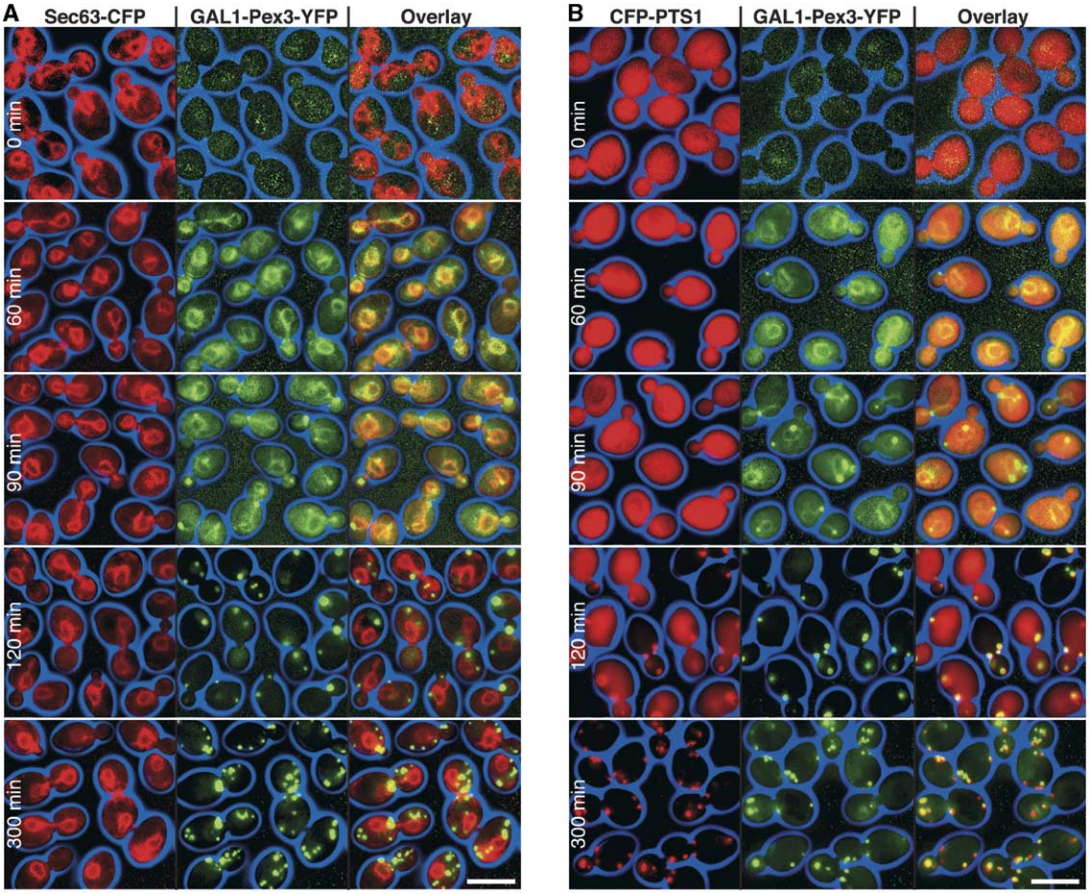

Figure 2. Pex3-YFP Trafficking during Peroxisome Development in *pex3Δ* Cells

(A) In cells labeled for the ER by Sec63-CFP, no Pex3-YFP signal is detectable at onset of induction (0 min). The perinuclear ER is apparent as a thin ring structure. Sixty minutes later, the first detectable, weak Pex3-YFP signal localizes into structures that colocalize with the ER marker Sec63-CFP. Ninety minutes after induction, Pex3-YFP starts to concentrate into dots frequently localized on or at the periphery of the ER, apparent in the overlay panel. One hundred and twenty minutes after induction, the Pex3-YFP dots are significantly brighter and no longer overlap with the Sec63-CFP signal. The weak ER labeling of Pex3 apparent at 60 min is no longer detectable. At 300 min, five to ten individual Pex3-YFP dots per cell are discernible that show no apparent ER colocalization but mostly localize to the cell cortex as observed for peroxisomes in wild-type cells. Scale bar, 5 μm.

(B) At the onset of the Pex3-YFP time-course experiment, no Pex3-YFP signal is detectable. Exclusively cytoplasmic CFP-PTS1 demonstrates the absence of import-competent peroxisomes. Despite discernible Pex3-YFP signal 60–90 min after induction, CFP-PTS1 is still uniformly cytoplasmic, indicating that no import-competent peroxisomes have been formed yet. The formation of bright, dot-like Pex3-YFP structures at 120 min is accompanied by onset of PTS1 import, discernible by accumulation of CFP-PTS1 signal into dots overlapping with the speckles marked by Pex3-YFP. At 300 min, the cytoplasmic background of CFP-PTS1 drops below detection level, and the protein is exclusively localized at Pex3-YFP marked dots, indicating that mature, import-competent peroxisomes have been restored. Scale bar, 5 μm.

their migration behavior in one blot assay: Sec63-CFP (95 kDa), Pex3-YFP (77 kDa), and CFP-PTS1 (27 kDa). In the absence of Mg^{2+}, Sec63-CFP and Pex3-YFP cofractionate (Figure 3A). CFP-PTS1 is present in the top fractions due to the absence of peroxisomes as observed by microscopy at this time point (Figure 2B). These top fractions do not contain Pex3-YFP, indicating the absence of a cytoplasmic pool of Pex3-YFP. In the gradient containing Mg^{2+}, both Sec63-CFP and Pex3-YFP shifted to the bottom fractions of the gradient without loss of colocalization (Figure 3B). The preservation of the distribution pattern strongly supports the notion that Pex3-YFP and Sec63-CFP share the same organellar compartment: the ER. As expected, the location of cytosolic CFP-PTS1 remains the same in the Mg^{2+}-containing gradient, and again, there is no evidence for the presence of any cytosolic Pex3-YFP.

As a control to demonstrate the specificity of the coordinated density shift, we followed the behavior of mitochondria in the gradients using Tim44 as a marker protein. Mitochondria show the opposite behavior: in the presence of Mg^{2+}, mitochondria shift to a lower equilibrium density. This result underlines the importance of the observed match between Sec63-CFP and Pex3-YFP distribution patterns in the two different conditions.

Combining these observations and taking into account that both Sec63 and Pex3 are integral membrane proteins, we conclude that, after induction, Pex3 first targets to the ER, concentrates into ER substructures,

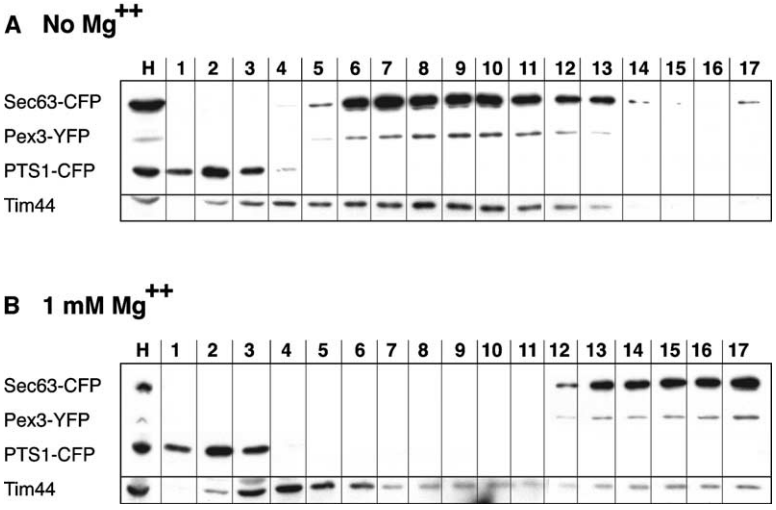

Figure 3. Cofractionation of Pex3-YFP and Sec63-CFP under Varying Conditions with and without Mg^{2+} during Sucrose-Density-Gradient Centrifugation

Cells were harvested 90 min after induction, and postnuclear supernatants were prepared, one in buffer containing 1 mM Mg^{2+}, the other in buffer containing 10 mM EDTA. The supernatants were analyzed by sucrose-density-gradient centrifugation, and 17 fractions were taken for Western blot inspection using an antibody against GFP. The behavior of mitochondria was followed on the basis of Tim44 as marker protein. H indicates the homogenate; lane 1 is the top fraction; lane 17 is the bottom fraction.

and separates from the ER in precompartments that subsequently mature into organelles capable of importing a PTS1 marker protein, indicating that bona fide peroxisomes represent the end station of its trafficking route.

YFP-Pex3 Also Travels via the ER in Wild-Type Cells

We have repeated the time-course experiment in strains with a wild-type *PEX3* gene (DHY842 and DHY844). Now the YFP-Pex3 protein produced after induction can choose between two organelles: the ER and the peroxisomes already present. These peroxisomes are marked with the constitutively expressed CFP-PTS1. Again, YFP-Pex3 accumulated first in the ER before arriving into the peroxisomes (Figure 4). This result underscores two important points. (1), the appearance of Pex3 in the ER is not a matter of mistargeting. When fully competent peroxisomes are available, Pex3 still goes first to the ER before showing up in peroxisomes. (2), the appearance of Pex3 in the ER of a peroxisome-less strain does not represent an adaptive response that is only followed in a situation where peroxisomes are not initially present. This experiment demonstrates that targeting of Pex3 to the ER prior to its appearance in peroxisomes is a normal feature of a wild-type cell.

Pex19 Is Required for Exit of Pex3 from the ER

Both Pex3 and Pex19 are required for recruiting membrane proteins to the peroxisome, and both *pex3* or *pex19* mutants have no peroxisomes or remnants thereof (Erdmann et al., 1989; Fang et al., 2004; Götte et al., 1998; Hettema et al., 2000; Höhfeld et al., 1991; Jones et al., 2004; Sacksteder et al., 2000). We therefore determined the fate of Pex3 in the absence of Pex19. For this, we repeated the Pex3 induction experiments in strains lacking *PEX19*. The *GAL1*-inducible Pex3 as the sole source of Pex3 protein was labeled with YFP at either the N or the C terminus (*GAL1-PEX3-YFP* [DHY819 and DHY839] or *GAL1-YFP-PEX3* [DHY848 and DHY850] with either *SEC63-CFP pex3Δ pex19Δ* or *CFP-PTS1 pex3Δ pex19Δ*). Both Pex3-YFP as well as YFP-Pex3 (data not shown) colocalized with the Sec63-CFP-labeled ER after 60 min, as in the previous experiments. But in contrast to the previous experiments, Pex3 remained at the ER in the *pex19Δ* mutant, and no Pex3-containing dot localizing independently of Sec63-CFP or any mature peroxisome could ever be detected (Figure 5). Indefinite trapping of Pex3 at the ER was confirmed in cells where production of low levels of YFP-Pex3 was prolonged for more than 16 hr. We conclude that Pex19 function is required for the formation of Pex3-containing membrane structures; without Pex19p, Pex3 cannot exit the ER.

Pex19 Localizes First to Subregions of the ER

Pex19 is a (predominantly) cytosolic protein, although some controversy exists about its partial binding to subcellular structures (Götte et al., 1998; Hettema et al., 2000; Jones et al., 2004; Sacksteder et al., 2000; Snyder et al., 2000). Its interaction with the membrane protein Pex3 indicates the possibility of finding Pex19 somewhere along the trafficking route of Pex3. Moreover, our observation that YFP-Pex3 was trapped into the ER in the absence of Pex19 raised the question of whether we could confirm a role for Pex19 in the exit of Pex3 from the ER.

To assess this, we constructed *GAL1-YFP-PEX19*-inducible strains and performed time courses similar to those with Pex3 (Figure 6, strains DHY845 and DHY847). The cells lost all detectable peroxisomes upon growth on glucose, as illustrated by the cytoplasmic localization of the two peroxisomal-membrane proteins Pex1 and Pex15 (data not shown). Shortly after induction, YFP-Pex19 staining indeed was absent, and CFP-PTS1 showed exclusive cytosolic localization (Figure 6B). After 60 min, we observed uniform cytoplasmic localization of YFP-Pex19, without any detectable concentration at specific sites. However, 90 min after induction, a dot-like signal arose that localized close to or onto the ER. After 120 min, YFP-Pex19 dots appeared to be randomly localized, and their number increased (comparable to the Pex3-YFP time courses). Finally, after 300 min, CFP-PTS1 was completely im-

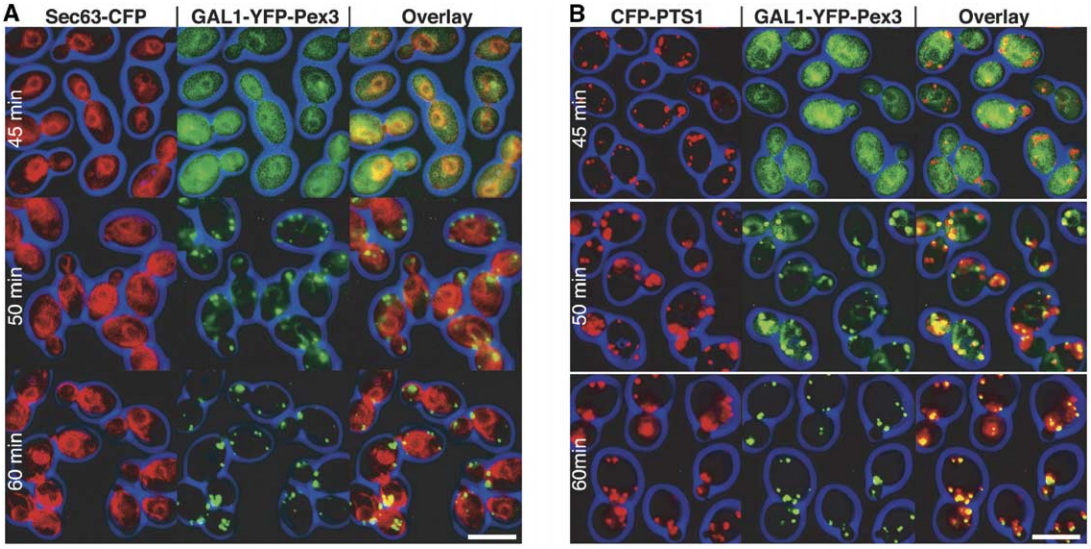

Figure 4. YFP-Pex3 Shuttles via the ER in Wild-Type Cells Containing Peroxisomes

Forty-five minutes after limited induction of *GAL1-YFP-PEX3*, very weak YFP-Pex3-labeled structures can be observed before YFP-Pex3 localizes to the existing peroxisomes. The structures colocalize with the ER marker Sec63-CFP, demonstrating the first detectable localization of YFP-Pex3 to be the ER as depicted in (A). Wild-type peroxisomes marked with CFP-PTS1 in (B) remain largely unlabeled by YFP-Pex3 at this early time point, but few colocalizing dots are discernible in few cells. Already, 5 min later, only very weak ER-localized YFP-Pex3 can be detected (A), but substantial amounts of the Pex3-YFP signal concentrate into the CFP-PTS1-labeled peroxisomes (B). Sixty minutes after limited induction, all detectable YFP signal is organized in ER-independent dots (A) marked as peroxisomes by the CFP-PTS1 label (B). Scale bars, 5 μm.

ported into the newly formed peroxisomes, and part of the YFP-Pex19 colocalized with the new organelles, while the rest remained cytosolic. The initial concentration of Pex19 into dots at the ER supports the notion that the earliest events in peroxisome formation occur at the ER.

Pex3 Is Required for Anchoring Pex19p to Subregions of the ER

The concentration of Pex19 at the ER 90 min after induction spatially and temporally coincides with the pattern observed for Pex3 in the previous time courses (Figures 2 and 6). To show that it is indeed the membrane protein Pex3 that recruits part of the cytosolic pool of Pex19 into dots at the ER membrane, we studied the behavior of YFP-Pex19 after induction in the absence of Pex3 (*pex3Δ*). We constructed the corresponding *pex3* null mutants in the CFP-PTS1 and Sec63-CFP-labeled *GAL1-YFP-PEX19* strains and repeated the time course (Figure 7, strains DHY846 and DHY849). The YFP-Pex19 signal only localized to the cytosol and never concentrated into the ER-associated dot-like structure. As a consequence, cells did not develop peroxisomes.

We conclude that ER-localized Pex3 attracts Pex19 and marks the site for insertion of additional peroxisomal-membrane proteins, allowing the next steps in peroxisome development to take place.

Discussion

We have shown that the endoplasmic reticulum contributes to the formation of peroxisomes. This concept is based on our observations in *S. cerevisiae* that the two peroxisomal proteins required for peroxisomal membrane biogenesis, Pex3 and Pex19, both target first to the ER before appearing in peroxisomes. Real-time imaging of YFP/CFP-tagged proteins using the fluorescence microscope revealed the following morphological features: shortly after synthesis, the fluorescence signal of Pex3-YFP completely overlaps with the

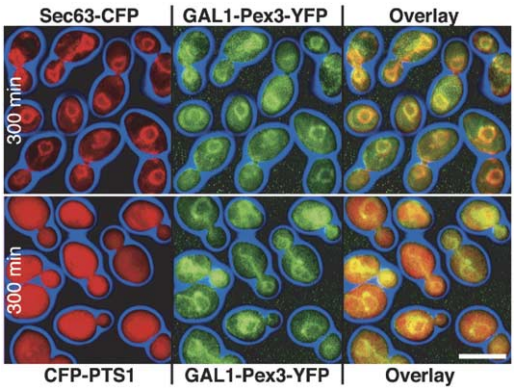

Figure 5. Pex3-YFP Trafficking during Peroxisome Formation in *pex3Δ pex19Δ* Cells

In contrast to *pex3Δ* cells shown in Figure 2, in *pex3Δ pex19Δ* cells, even 300 min after limited induction of Pex3-YFP, still all YFP signal overlaps with the ER as marked by Sec63-CFP, shown in the upper panel. No dot-like Pex3-YFP structure is formed. Import-competent peroxisomes are completely absent, as depicted by the uniformly cytoplasmic CFP-PTS1 signal shown in the lower panel. Scale bar, 5 μm.

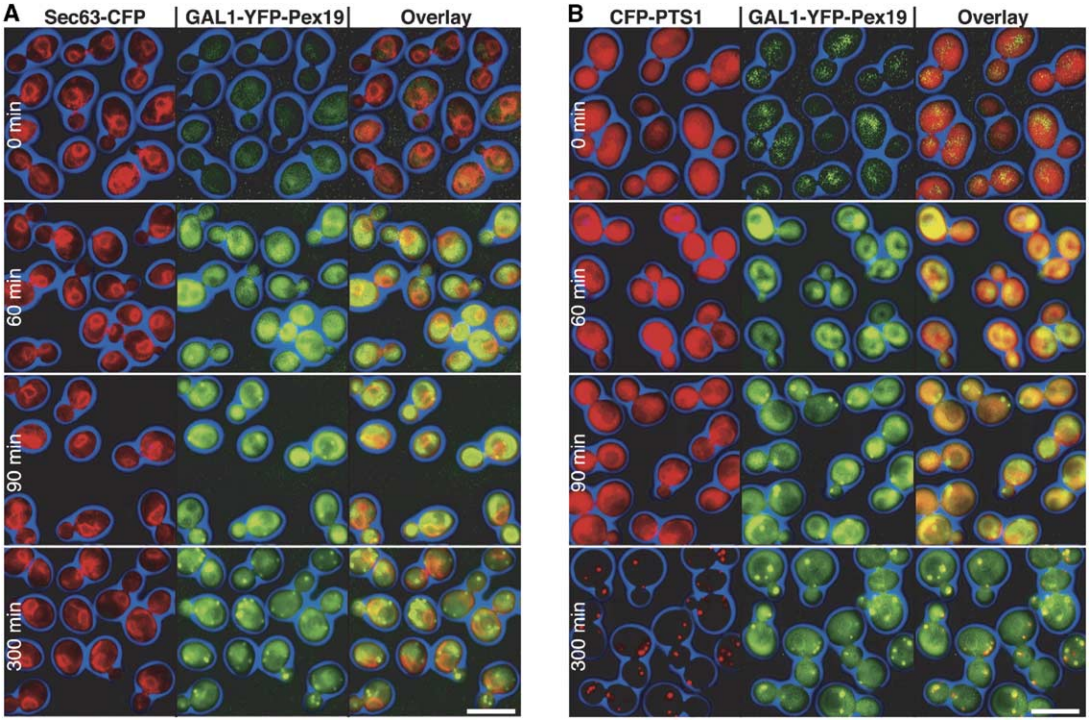

Figure 6. YFP-Pex19 Trafficking during Peroxisome Formation

(A) In cells labeled for the ER by Sec63-CFP with the only source of Pex19 under control of the *GAL1* promoter, no YFP-Pex19 signal is detectable at the beginning of induction (0 min). Sixty minutes later, a cytoplasmic pool of YFP-Pex19 is detectable that is excluded from the nucleus and the vacuoles. No apparent enrichment at the ER periphery can be detected. At 90 min, in addition to the cytoplasmic pool of Pex19, concentration into one or few dots becomes apparent. Colocalization analysis shows the dots to be located on or at the ER periphery. At 300 min, the cytoplasmic pool of Pex19-YFP is still present; in addition, so are five to ten individual YFP-Pex19 dots per cell. The enriched dots show no apparent ER colocalization but mostly localize to the cell cortex as observed for peroxisomes in wild-type cells. Scale bar, 5 μm.

(B) At the beginning of induction, uniformly cytoplasmic CFP-PTS1 signal demonstrates the complete lack of import-competent peroxisomes in cells with the only source of Pex19 under control of the *GAL1* promoter. Also, no YFP-Pex19 signal is detectable at the beginning of induction. Sixty minutes later, a cytoplasmic pool of YFP-Pex19 is detectable, but CFP-PTS1 import cannot be observed. At 90 min, YFP-Pex19 accumulates in one or few dots, but CFP-PTS1 remains uniformly cytoplasmic. At 300 min, the cytoplasmic background of CFP-PTS1 drops below detection level, and the protein is exclusively localized in dots, indicating that import-competent peroxisomes have been restored. The dots colocalize with the bright speckles of YFP-Pex19, showing that YFP-Pex19 remains enriched on mature peroxisomes. Scale bar, 5 μm.

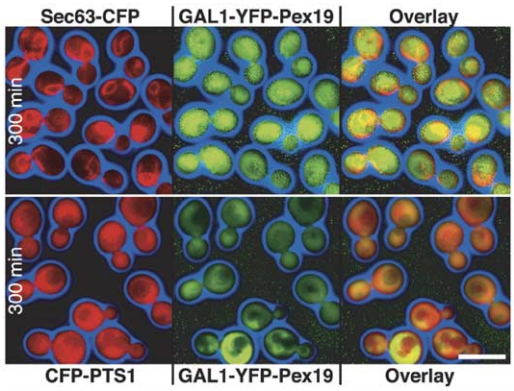

Figure 7. YFP-Pex19 Remains Uniformly Cytoplasmic in the Absence of Pex3

In the absence of Pex3, YFP-Pex19 fails to enrich in punctate structures that show colocalization with the ER (upper panel) or mature peroxisomes, as no PTS1 import-competent peroxisomes are ever formed (lower panel).

Sec63-CFP-labeled ER. Both are integral membrane proteins (Feldheim et al., 1992; Höhfeld et al., 1991), and we conclude that they share the same membrane: the perinuclear and cortical ER. This is corroborated by biochemical experiments in which we showed that Pex3 and Sec63 coshift in a sucrose density gradient depending on the Mg^{2+} concentration. Next, Pex3-YFP concentrates into one or two fluorescent dot-like structures located close to or still associated with the ER membrane. At this stage, part of YFP-Pex19 becomes localized into similar dot-like structures, while the rest remains in the cytosol. Previous characterization of Pex3 and Pex19 indicates that both proteins physically interact (Götte et al., 1998; Ito et al., 2001) and share the same function: recognition and insertion of newly synthesized proteins into the peroxisomal membrane (Hettema et al., 2000; Fang et al., 2004; Jones et al., 2004). We therefore conclude that Pex3 and Pex19 reside in the same dot-like structures, in which Pex3 serves as the anchor protein onto which Pex19 docks. Shortly after, the close association of these dot-like structures with the ER is lost, and the capacity to import proteins starts as part of the cytosolic CFP-PTS1

coincides with the Pex3-YFP-marked dots. Finally, multiple peroxisomes arise that have taken up all of the CFP-PTS1 from the cytosol.

This sequence of events is the same in two genetically different contexts: the *pex3Δ* mutant, in which the full complement of peroxisomes needs to be restored, and wild-type cells, in which peroxisomes are already present when Pex3-YFP synthesis is initiated. Only the timing is different. In wild-type cells, the residence time of Pex3-YFP in the ER is shorter and more difficult to capture. This is probably due to the fact that all of the components supporting the routing from ER to peroxisomes are in full operation in wild-type cells, while they must be reinstalled in mutant cells lacking peroxisomes. The congruence of results between mutant and wild-type cells underscores the ER contribution to peroxisome biogenesis as required and operational under all conditions of cellular life.

It is understandable that an ER-localized pool of Pex3 has not been detected previously. The Pex3 concentration in the ER appears to be significantly lower than the one in mature peroxisomes. Before Pex3-YFP appears in peroxisomes, we registered a signal-to-background ratio of 0.05 in the ER. But a ratio of 1.38 was measured for the peroxisome-localized pool of Pex3 (see Experimental Procedures). Thus, detection of the ER-localized Pex3 was already very difficult in our pulse-chase approach and could only be achieved using a very sensitive CCD camera (see Experimental Procedures). But the strong signal difference makes it technically almost impossible to detect the ER-localized Pex3-YFP signal by epifluorescence microscopy under steady-state conditions in the presence of mature, Pex3-YFP-labeled peroxisomes. This difference in concentration also hinders localization of Pex3 by biochemical fractionation experiments. It would be impossible to judge if a small amount of Pex3 in the ER fraction would be contamination or correct localization.

The observations of colocalization and interaction of Pex3 and Pex19 are in agreement with previous reports (Hettema et al., 2000; Fang et al., 2004; Jones et al., 2004). New is the subcellular location at which both proteins start their biological function. Thus far, their role was surmised to be at the peroxisomal membrane only. The novel localization of Pex3 and Pex19 to the ER membrane and the observed formation of Pex3- and Pex19-containing dot-like structures at the ER are in perfect agreement with the observed complete lack of peroxisomal membrane structures upon loss of either Pex3 or Pex19. Involvement of the ER in formation of the peroxisomal membrane is further supported by the localization of Pex3 and Pex19 in the absence of the interacting partner: without Pex19, Pex3 is trapped in the ER and no vesicle is formed. Complementarily, without Pex3 present, Pex19 fails to dock to the ER membrane, and, again, no peroxisomal precompartment is formed.

Our interpretation of the results based on a pulse-chase-like approach in live *S. cerevisiae* cells is in line with other observations linking the ER to peroxisome formation. Very recently, Emp24, the integral component of endoplasmic reticulum-derived COPII-coated vesicles, which function in ER-to-Golgi transport, has been detected on nascent peroxisomes in budding yeast (Marelli et al., 2004; Otte et al., 2001). In *Yarrowia lipolytica*, the peroxisomal proteins Pex2 and Pex16 are N-glycosylated, indicating that they passed the ER (Titorenko et al., 1997), and in a conditional *pex3* mutant, ER-associated vesicular structures appeared, but their role in peroxisome biogenesis remained unclear (Bascom et al., 2003). In mouse dendritic cells, the development of peroxisomes was described in morphological terms using the electron microscope (Geuze et al., 2003; Tabak et al., 2003). These cells show remarkable intermediate stages of peroxisome development in which the occurrence of Pex proteins could be demonstrated by decoration with gold particles. Our dynamic yeast light-microscope data compare well with the mammalian pictures obtained by electron microscopy. In the mouse cells, Pex13 was found in specialized regions of the ER. These could be similar to the yeast dot-like structures that are still associated with the ER. This is in agreement with recent findings that, also in yeast, Pex13-YFP can be observed in or at the ER in the absence of Pex3 and Pex19 (unpublished data). This congruence in observations between two widely diverged species, a fungal cell compared to a mammalian cell, stresses the generality of the new concept that the ER contributes to peroxisome formation.

Our novel model for peroxisome formation raises but also clarifies a number of questions. Pex3 robustly targets to the ER regardless of whether the N or C terminus is masked with YFP, and our Western blot analysis detected one band of appropriate size for Pex3 only. Thus, it appears not to be processed, and its amino acid sequence lacks telltale marks of how it gets there, such as a detectable signal peptide. Pex3 is in this respect an example of a larger group of ER proteins for which it is equally unknown how they reach the ER (reviewed by Borgese et al., 2003). Attempts to implicate the ER in peroxisome formation were mainly based on principles delineated for the vesicle trafficking route followed by secretory proteins. Thermosensitive mutants impairing the function of the Sec61 protein import channel in *S. cerevisiae* showed no impairment of peroxisome formation after shifting the cells to the nonpermissive temperature (South et al., 2001). However, the Sec61 complex may not be used at all for the insertion of the few peroxisomal proteins entering the ER. The morphological data from yeast and dendritic cells indicate that relatively large portions of the ER are captured for peroxisome development. This may be supported by factors that differ from the ones involved in small-vesicle formation and trafficking. Genetic screens in a number of yeast species and CHO cells revealed 31 genes involved in various aspects of peroxisome formation. However, none of these revealed a direct clue to involvement of the ER. This may be due to the fact that the design of the screens did not allow for identification of essential genes. It is likely that the ER-specific proteins involved in the uptake of peroxisomal proteins are also required for uptake of ER proteins with essential functions, thus preventing their recognition in screens applied thus far. An example of such an essential household protein is the recent discovery of the contribution of Rho1 to peroxisome maintenance (Marelli et al., 2004).

Interesting new questions come to mind. Prior to sequestering part of the ER membrane, care must be taken to separate resident ER proteins from the peroxisomal proteins because each compartment retains its protein signature. This is particularly well illustrated by the distribution of chaperones. Although most intracellular compartments have their share of chaperones, such proteins have not been found in peroxisomes (Kikuchi et al., 2004). Apparently the abundant group of ER chaperones is kept well away from the ER regions that are destined for peroxisome formation.

Peroxisomes are often grouped together with mitochondria and chloroplasts on the assumption that all three originated from endosymbionts in a primitive eukaryotic cell (Alberts et al., 2002). Our new findings resolve certain differences and problems that are ignored when the three types of organelles are grouped together. Mitochondria and chloroplasts are bound by multiple membranes and contain DNA; peroxisomes are surrounded by a single limiting membrane and lack DNA. With the new insight that peroxisomes derive their membrane from the ER, these differences are explained.

In the traditional grouping, an important problem for all three organelles is how lipids are acquired to enlarge the surface area of their membranes. In many cases, the lipids needed are synthesized in different subcellular compartments. This raises the important question of how the lipids are transported between organelles. For mitochondria and chloroplasts, a favored hypothesis is that membranes come into close association, allowing lipid transfer to take place (reviewed by Daum and Vance, 1997; Voelker, 2000). Our results indicate that peroxisomes rely on a completely different mechanism: they recruit their membrane directly from the ER. This also explains the enigma of how peroxisomes can be restored in cells that lack peroxisomes and have been without them for many generations. They can always be regenerated as long as a functional ER is available.

Our findings may also reinvigorate speculation about the evolutionary origin of peroxisomes. Peroxisomal enzymes, mostly oxidases with inefficient energy-conserving properties, are considered to be primitive examples of a long evolutionary past when the reducing atmosphere of the earth changed into an oxidative one. As a consequence, the organelles containing them might have been among the first of the developing cytomembrane system in the primitive eukaryotic cell. The origin of the peroxisomal membrane from the ER is in line with this scenario and makes it less likely that the organelles have an endosymbiotic origin. Indeed, proteins involved in peroxisome formation and maintenance (the peroxins) show typical eukaryotic protein motifs (TPR, WD-40, AAA, RING, and SH3 domains), which supports the notion that peroxisomes are an invention of the primitive eukaryote itself. An intriguing question is why and how peroxisomes developed their own protein import machinery enabling them to take up proteins synthesized in the cytosol. Hopefully, with the availability of more and more sequenced genomes of organisms of all sorts, comparative genomics can come up with some of the answers to how peroxisomes developed in evolutionary times.

Experimental Procedures

DNA Manipulations, Cloning Procedures, and Strain Constructions

Yeast strains used in this study are listed in Table S1. We applied a PCR-based method to construct gene deletion cassettes and CFP/YFP-fusion or *GAL1*-fusion cassettes for transformations (Wach et al., 1994). Oligos are depicted in Table S2. DNA of *E. coli* plasmids pFA6-HisMX6 (Wach et al., 1994), pYM3 (Knop et al., 1999), pDH3, and pDH5 (Yeast Resource Center, University of Washington, Seattle) and pFA6KanMX6-PGAL1 and a pFA6KanMX6-PGAL1-GFP (Longtine et al., 1998) variant with the GFP exchanged for YFP served as template for preparative PCR reactions. Genomic integration of the corresponding construct was verified by analytical PCR (Huxley et al., 1990; Wach et al., 1994). Plasmid pEW171 containing CFP-PTS1 that highlights peroxisomes (Hettema et al., 1998; Monosov et al., 1996) was constructed as described in Hoepfner et al. (2001). The *GAL1-PEX3-YFP* integration plasmid (pDHsb1) was constructed as follows: the *GAL1* promoter was amplified by PCR from pFA6a-kanMX6-PGAL1 using oligonucleotides introducing flanking EcoRI and SacI sites. The fragment was cloned into the corresponding sites of Yiplac128 (Gietz and Sugino, 1988). *PEX3-YFP* was amplified from the genomic DNA from strain DHY486 using oligos that introduced BamHI and HindIII sites. The fragment was cloned into the corresponding sites. As we had previously introduced a spacer between the SacI and BamHI site, the spacer was excised with SacIxBamHI and the DNA ends were blunted with mung-bean nuclease and ligated. The plasmid was sequenced and tested. Plasmid GAL1-PEX3-mYFP was constructed by PCR amplification of YFP from plasmid pDH5 with primers mYFP p1 and p2. Both primers introduced a flanking XmaI site. The long primer p2 contained the carboxy terminus of YFP starting at D216 and replaced the codon for L221 (CTT) into K221 (AAG). The PCR product was cut with XmaI and ligated into plasmid pGAL1-PEX3-XmaI, where, by introduction of the codon for glycine GGG just before the stop codon, an XmaI site had been created. The resulting construct was pGAL1-PEX3-mYFP (pDHsb1mYFP). The plasmid was sequenced and tested.

Western Blot Analysis

Ten OD units of yeast cells were lysed by vigorous vortexing for 10 min in the presence of 0.5 mm glass beads (Biospec Products) at 4°C. The homogenate was assessed for its protein concentration by Bradford analysis (Bio-Rad). Thirty micrograms of protein was subjected to SDS-PAGE on a 10% gel and transferred onto nitrocellulose membrane (Amersham Bioscience). The membrane was probed with primary mouse anti-GFP antibody 1814460 (Roche) followed by a secondary anti-mouse antibody conjugated with horseradish peroxidase (Jackson Immunoresearch) and detected by ECL system (Amersham Bioscience). The blot was subsequently stripped for 30 min at 60° in stripping buffer (2% SDS, 62.5 mM Tris [pH 6.8], 100 mM β-mercaptoethanol), washed, and reprobed with primary rat antibody against β-tubulin, YOL34 (Serotec), followed by a secondary anti-rat antibody conjugated with horseradish peroxidase (Jackson Immunoresearch) and detected again by ECL system (Amersham Bioscience).

ER Shift Assay

Cells were grown as for the time courses described in the next section. At time point 90 min, fractionation and equilibrium-density-gradient centrifugation were performed as described by Roberg et al. (1997). After initial washing steps, 4×10^8 cells were resuspended in 0.5 ml STE (10% w/v sucrose, 10 mM Tris-Cl [pH 7.4], and 10 mM EDTA), and 4×10^8 cells were resuspended in ST (10% w/v, 10 mM Tris-Cl [pH 7.4], and 1 mM $MgCl_2$). After glass-bead lysis and centrifugation, the resulting postnuclear supernatants were diluted to 1 ml with either STE or ST. Three hundred microliters of each supernatant was layered on top of a 5 ml linear 20%–40% w/v sucrose gradient made up in ST or STE, respectively, and spun to equilibrium for 14 hr at 100,000 × g. Seventeen fractions of

300 μl (together equivalent to the input supernatant) were collected starting from the top of the gradient using a micropipette. Fractions and 300 μl of both postnuclear supernatants were diluted with TCA to 1.4 ml with a final TCA concentration of 10% w/v and pelleted by centrifugation for 45 min at 20,000 × g. Protein pellets were washed once with 5% TCA and twice with acetone. The pellets were subjected to SDS-PAGE on a 10% gel and transferred onto nitrocellulose membrane (Amersham Bioscience). Sec63-CFP, Pex3-YFP, and YFP-PTS1 were detected as described above. Tim44 was detected by probing the membrane with an anti-Tim44 antibody after stripping the blot in stripping buffer (see above).

Image Acquisition and Processing

The microscopy system setup has been described previously (Hoepfner et al., 2001). Strains for time courses and ER shift assays were grown in YP-2% glucose medium to mid-log phase, diluted 10 times in YP-4% raffinose medium, and grown again to mid-log phase at 30°C. The cells were spun down and resuspended in an equal volume of YP-2% galactose for 30 min, then washed in dH_2O and taken up in the double volume of YP-4% glucose. For prolonged limited expression from the *GAL1* promoter, cells were shifted to YP-1.8% glucose/0.4% galactose 5 hr later. For microscopy, the cells were washed with PBS, and 3 μl of the culture was spread on a poly-L-lysine-treated slide overlaid with a coverslip and immediately used for microscopy. We acquired one phase-contrast image and 3 z axis planes spaced by 0.8 μm. In each z axis plane, we acquired one YFP and one CFP image with 2 s exposure times and 100% fluorescence transmission. Each individual plane was then processed using the "remove haze" command of Metamorph (Universal Imaging Corp.). Separately, the YFP and CFP images were then merged into one plane using the "stack arithmetic: maximum" command. These planes were used for intensity measurements described below. For presentation in figures, the YFP/CFP planes were scaled and converted to 8-bit images. The drastic difference in Pex3 signal intensity during the induction time courses made it necessary to scale individual time points of a time course differently (as apparent by the intensity differences of the background). The phase-contrast, YFP, and CFP images were overlaid, with default color-balance settings assigning false-color look-up tables. Blue color was applied to the phase-contrast picture, green color to the YFP channel, and red to the CFP channel. Representative cells were selected and assembled into panels using Adobe Photoshop (Adobe Systems). Intensity measurements for dot-like signals were done by identifying the brightest pixel in the dot and recording the absolute gray level. Intensity of dispersed signals like perinuclear ER was measured by registering the absolute gray level of five randomly selected pixels. Absolute gray levels were then normalized against the background signal. The background signal was determined by selecting a 100 × 100 pixel region on the picture plane not containing cells and calculating the average gray level using the "region statistic" command of Metamorph.

Supplemental Data

Supplemental Data include five figures and two tables and can be found with this article online at http://www.cell.com/cgi/content/full/122/1/85/DC1/.

Acknowledgments

We are grateful to E. Hettema for the CFP-PTS1 plasmids and to A. van der Zand, S. Helliwell, A. Gladfelter, and M. Hall for critical reading of the manuscript and stimulating suggestions. This work was supported by a grant from the Academic Biomedical Centre of the University of Utrecht to H.F.T. and by grants of the University of Basel and a European Molecular Biology Organization fellowship to D.H. (EMBO LTF 505-2001).

Received: December 13, 2004
Revised: March 15, 2005
Accepted: April 25, 2005
Published: July 14, 2005

References

Alberts, B., Johnson, A., Lewis, J., Raff, M., Roberts, K., and Walter, P. (2002). Molecular Biology of the Cell (New York: Garland Science Publishing).

Bascom, R.A., Chan, H., and Rachubinski, R.A. (2003). Peroxisome biogenesis occurs in an unsynchronized manner in close association with the endoplasmic reticulum in temperature-sensitive *Yarrowia lipolytica* Pex3p mutants. Mol. Biol. Cell *14*, 939–957.

Borgese, N., Colombo, S., and Pedrazzini, E. (2003). The tale of tail-anchored proteins: coming from the cytosol and looking for a membrane. J. Cell Biol. *161*, 1013–1019.

Daum, G., and Vance, J.E. (1997). Import of lipids into mitochondria. Prog. Lipid Res. *36*, 103–130.

de Duve, C. (1996). The birth of complex cells. Sci. Am. *274*, 50–57.

Erdmann, R., Veenhuis, M., Mertens, D., and Kunau, W.H. (1989). Isolation of peroxisome-deficient mutants of Saccharomyces cerevisiae. Proc. Natl. Acad. Sci. USA *86*, 5419–5423.

Fang, Y., Morrell, J.C., Jones, J.M., and Gould, S.J. (2004). *PEX3* functions as a *PEX19* docking factor in the import of class I peroxisomal membrane proteins. J. Cell Biol. *164*, 863–875.

Fehrenbacher, K.L., Davis, D., Wu, M., Boldogh, I., and Pon, L.A. (2002). Endoplasmic reticulum dynamics, inheritance, and cytoskeletal interactions in budding yeast. Mol. Biol. Cell *13*, 854–865.

Feldheim, D., Rothblatt, J., and Schekman, R. (1992). Topology and functional domains of Sec63p, an endoplasmic reticulum membrane protein required for secretory protein translocation. Mol. Cell. Biol. *12*, 3288–3296.

Geuze, H.J., Murk, J.L., Stroobants, A.K., Griffith, J.M., Kleijmeer, M.J., Koster, A.J., Verkleij, A.J., Distel, B., and Tabak, H.F. (2003). Involvement of the endoplasmic reticulum in peroxisome formation. Mol. Biol. Cell *14*, 2900–2907.

Gietz, D.R., and Sugino, A. (1988). New yeast-*Escherichia coli* shuttle vectors constructed with *in vitro* mutagenized yeast genes lacking six base pair restriction sites. Gene *74*, 527–534.

Götte, K., Girzalsky, W., Linkert, M., Baumgart, E., Kammerer, S., Kunau, W.H., and Erdmann, R. (1998). Pex19p, a farnesylated protein essential for peroxisome biogenesis. Mol. Cell. Biol. *18*, 616–628.

Hettema, E.H., Ruigrok, C.C., Koerkamp, M.G., van den Berg, M., Tabak, H.F., Distel, B., and Braakman, I. (1998). The cytosolic DnaJ-like protein Djp1p is involved specifically in peroxisomal protein import. J. Cell Biol. *142*, 421–434.

Hettema, E.H., Girzalsky, W., van Den Berg, M., Erdmann, R., and Distel, B. (2000). *Saccharomyces cerevisiae* Pex3p and Pex19p are required for proper localization and stability of peroxisomal membrane proteins. EMBO J. *19*, 223–233.

Hoepfner, D., van den Berg, M., Philippsen, P., Tabak, H.F., and Hettema, E.H. (2001). A role for Vps1p, actin, and the Myo2p motor in peroxisome abundance and inheritance in *Saccharomyces cerevisiae*. J. Cell Biol. *155*, 979–990.

Höhfeld, J., Veenhuis, M., and Kunau, W.H. (1991). *PAS3*, a *Saccharomyces cerevisiae* gene encoding a peroxisomal integral membrane protein essential for peroxisome biogenesis. J. Cell Biol. *114*, 1167–1178.

Huxley, C., Green, E.D., and Dunham, I. (1990). Rapid assessment of *S. cerevisiae* mating type by PCR. Trends Genet. *6*, 236.

Ito, T., Chiba, T., Ozawa, R., Yoshida, M., Hattori, M., and Sakaki, Y. (2001). A comprehensive two-hybrid analysis to explore the yeast protein interactome. Proc. Natl. Acad. Sci. USA *98*, 4569–4574.

Jones, J.M., Morrell, J.C., and Gould, S.J. (2004). *PEX19* is a predominantly cytosolic chaperone and import receptor for class 1 peroxisomal membrane proteins. J. Cell Biol. *164*, 57–67.

Kikuchi, M., Hatano, N., Yokota, S., Shimozawa, N., Imanaka, T., and Taniguchi, H. (2004). Proteomic analysis of rat liver peroxisome: presence of peroxisome-specific isozyme of Lon protease. J. Biol. Chem. *279*, 421–428.

Knop, M., Siegers, K., Pereira, G., Zachariae, W., Winsor, B., Nasmyth, K., and Schiebel, E. (1999). Epitope tagging of yeast genes using a PCR-based strategy: more tags and improved practical routines. Yeast *5*, 963–972.

Lazarow, P.B. (2003). Peroxisome biogenesis: advances and conundrums. Curr. Opin. Cell Biol. *15*, 489–497.

Lazarow, P.B., and Fujiki, Y. (1985). Biogenesis of peroxisomes. Annu. Rev. Cell Biol. *1*, 489–530.

Lisenbee, C.S., Karnik, S.K., and Trelease, R.N. (2003). Overexpression and mislocalization of a tail-anchored GFP redefines the identity of peroxisomal ER. Traffic *4*, 491–501.

Longtine, M.S., McKenzie, A., Demarini, D.J., Shah, N.G., Wach, A., Brachat, A., Philippsen, P., and Pringle, J.R. (1998). Additional modules for versatile and economical PCR-based gene deletion and modification in *Saccharomyces cerevisiae*. Yeast *14*, 953–961.

Marelli, M., Smith, J.J., Jung, S., Yi, E., Nesvizhskii, A.I., Christmas, R.H., Saleem, R.A., Tam, Y.Y., Fagarasanu, A., Goodlett, D.R., et al. (2004). Quantitative mass spectrometry reveals a role for the GTPase Rho1p in actin organization on the peroxisome membrane. J. Cell Biol. *167*, 1099–1112.

Monosov, E.Z., Wenzel, T.J., Lüers, H.G., Heyman, J.A., and Subramani, S. (1996). Labeling of peroxisomes with green fluorescent protein in living *P. pastoris* cells. J. Histochem. Cytochem. *44*, 581–589.

Novikoff, P.M., and Novikoff, A.B. (1972). Peroxisomes in absorptive cells of mammalian small intestine. J. Cell Biol. *53*, 532–560.

Nunnari, J., and Walter, P. (1996). Regulation of organelle biogenesis. Cell *84*, 389–394.

Otte, S., Belden, W.J., Heidtman, M., Liu, J., Jensen, O.N., and Barlowe, C. (2001). Erv41p and Erv46p: new components of COPII vesicles involved in transport between the ER and Golgi complex. J. Cell Biol. *152*, 503–518.

Phillips, G.N. (1997). Structure and dynamics of green fluorescent protein. Curr. Opin. Struct. Biol. *7*, 821–827.

Roberg, K.J., Rowley, N., and Kaiser, C.A. (1997). Physiological regulation of membrane protein sorting late in the secretory pathway of *Saccharomyces cerevisiae*. J. Cell Biol. *137*, 1469–1482.

Rottensteiner, H., Kramer, A., Lorenzen, S., Stein, K., Landgraf, C., Volkmer-Engert, R., and Erdmann, R. (2004). Peroxisomal membrane proteins contain common Pex19p-binding sites that are an integral part of their targeting signals. Mol. Biol. Cell *15*, 3406–3417.

Sacksteder, K.A., Jones, J.M., South, S.T., Li, X.L., Liu, Y.F., and Gould, S.J. (2000). *PEX19* binds multiple peroxisomal membrane proteins, is predominantly cytoplasmic, and is required for peroxisome membrane synthesis. J. Cell Biol. *148*, 931–944.

Schliebs, W., and Kunau, W.H. (2004). Peroxisome membrane biogenesis: the stage is set. Curr. Biol. *14*, R397–R409.

Snyder, W.B., Koller, A., Choy, A.J., and Subramani, S. (2000). The peroxin Pex19p interacts with multiple, integral membrane proteins at the peroxisomal membrane. J. Cell Biol. *149*, 1171–1178.

South, S.T., Baumgart, E., and Gould, S.J. (2001). Inactivation of the endoplasmic reticulum protein translocation factor, Sec61p, or its homolog, Ssh1p, does not affect peroxisome biogenesis. Proc. Natl. Acad. Sci. USA *98*, 12027–12031.

Subramani, S. (1998). Components involved in peroxisome import, biogenesis, proliferation, turnover, and movement. Physiol. Rev. *78*, 171–188.

Tabak, H.F., Murk, J.L., Braakman, I., and Geuze, H.J. (2003). Peroxisomes start their life in the endoplasmic reticulum. Traffic *4*, 512–518.

Titorenko, V.I., Ogrydziak, D.M., and Rachubinski, R.A. (1997). Four distinct secretory pathways serve protein secretion, cell surface growth, and peroxisome biogenesis in the yeast *Yarrowia lipolytica*. Mol. Cell. Biol. *17*, 5210–5226.

van den Bosch, H., Schutgens, R.B., Wanders, R.J., and Tager, J.M. (1992). Biochemistry of peroxisomes. Annu. Rev. Biochem. *61*, 157–197.

Voelker, D.R. (2000). Interorganelle transport of aminoglycerophospholipids. Biochim. Biophys. Acta *1486*, 97–107.

Wach, A., Brachat, A., Pöhlmann, R., and Philippsen, P. (1994). New heterologous modules for classical or PCR-based gene disruptions in *Saccharomyces cerevisiae*. Yeast *10*, 1793–1808.

Warren, G., and Wickner, W. (1996). Organelle inheritance. Cell *84*, 395–400.

Zacharias, D.A., Violin, J.D., Newton, A.C., and Tsien, R.Y. (2002). Partitioning of lipid-modified monomeric GFPs into membrane microdomains of live cells. Science *296*, 913–916.